OXFORD UNIVERSITY

THE IONISATION LOSS OF RELATIVISTIC CHARGED PARTICLES IN THIN GAS SAMPLES AND ITS USE FOR PARTICLE IDENTIFICATION: II EXPERIMENTAL RESULTS

W.W.M. Allison, C.B. Brooks, J.N. Bunch, R.W. Pleming
R.K. Yamamoto

NUCLEAR PHYSICS LABORATORY

68/75

#20.

THE IONISATION LOSS OF RELATIVISTIC CHARGED PARTICLES IN THIN GAS SAMPLES AND ITS USE FOR PARTICLE IDENTIFICATION: II EXPERIMENTAL RESULTS

W.W.M. Allison, C.B. Brooks, J.N. Bunch, R.W. Pleming

Nuclear Physics Laboratory, Oxford.

R.K. Yamamoto, Massachusetts Institute of Technology, Cambridge, Massachusetts.

(Submitted for Publication in Nuclear Instruments and Methods.)

ABSTRACT

We present the results of an experiment in which a proportional chamber samples the ionisation loss of each incident relativistic particle some 60 times. The chamber, filled with 80% argon/20% CO_2 was exposed to a beam of pions, protons and electrons at momenta between 25 GeV/c and 150 GeV/c at the Fermi National Accelerator Laboratory. The observed pulse height spectra were corrected for systematic effects and compared with new Monte Carlo theoretical calculations discussed in paper I. The agreement is good. The relativistic rise is sufficient to enable individual pions and protons to be distinguished even with the present apparatus. Our results suggest that with a larger device kaons, pions and protons may be separated.

1. INTRODUCTION

In paper I[1] we reviewed the apparent discrepancy between theoretical and experimental results on the ionisation loss of relativistic charged particles in thin gas samples. We showed how using a more appropriate Monte Carlo calculation the discrepancy between theory and experiment could be resolved.

In this paper we present new experimental results which confirm the agreement between theory and earlier experiments and also demonstrate that individual particles of known momentum may be identified by their ionisation loss even using raw data. Particular attention is paid to systematic effects and calibration problems that could affect the predicted performance of a larger device[2].

In section 2 we describe the apparatus and in section 3 the energy calibration and factors affecting it. In section 4 we analyse the inter-channel correlation which is shown to be instrumental and to dominate the other sources of error in this case. Section 5 includes the experimental results and the comparison with theory.

2. THE APPARATUS

The experimental layout and chamber are shown in Fig. 1. The chamber was positioned downstream of a differential Cerenkov counter in the N3 beam line at the Fermi National Accelerator Laboratory. The tagged beam particles passed through the 120 cms long chamber parallel to a wire plane as shown in Fig. 1. This plane was sandwiched between two drift electrodes 7 cms apart and the whole mounted in a gas tight box which was flushed continuously with 80% argon/ 20% CO_2*. The ionisation electrons liberated by the incident particle are shown

---

* The gas mixture was chosen because of its convenience, large relativistic rise (Ref. 1) and properties as a drift chamber gas (Ref. 2,3).

symbolically as a row of dots in Fig. 1b drifting without amplification towards the central wire plane. The latter consists of pairs of 25μ diameter anode wires each separated by 250μ cathode wires to reduce capacitative cross coupling and to control the gas amplification. Each pair of anode wires collects and amplifies the electrons from 1.5 cms of gas and each such pulse is further amplified and integrated as discussed below. There were 60 such channels so that each particle traversing the detector yielded 60 pulse heights.

To achieve accurate spacing the wires were held in slots melted in perspex with a hot blade. The signal wires were connected in pairs to the input of the low impedance (20Ω) current sensitive preamplifiers, where typical signal amplitudes were a few μamps. The gas temperature and pressure were measured and recorded continuously by probes mounted in the box. In addition an Fe^{55} X-ray source was exposed between accelerator cycles to measure variations of the gas gain. It was placed in its shutter box above the chamber and shone through the aluminised mylar window of the gas box and through the upper foil drift electrode into the active region of the chamber. Typical counting rates were 20-30 per second. To calibrate the gain of the electronics, test pulses were sent to all channels in parallel from a current source.

The signals were carried from the preamplifiers to the receiver amplifiers in the control room by woven cables of balanced pairs. In the receiver amplifier units discriminator logic allowed the generation of self-triggers singly on a particular channel (for the X-ray source) or in coincidence between two chosen channels for beam particles. In addition each of the analogue signals was delayed by 200 nsecs and shaped to remove the long tail due to positive ion motion.[4] These signals were integrated in Lecroy 8-bit ADC channels with a 500 nsec gate to provide a pulse integral relatively insensitive to input pulse shape and trigger jitter. The ADC gate was triggered by the 2-channel coincidence occurring within the drift time (1 μsec) of a coincidence between the scintillator telescope (S1S2S3) and the particle identification signature required from the

differential Cerenkov counter. Triggers occurring within 2 μsecs of another S1S2S3 coincidence were rejected. The 500 nsec integration gate was fed in parallel to all ADCs. In addition to 57 standard data channels one only of the two data channels contributing to the coincidence was recorded.

The vector of 8 bit quantities together with a status register was read from CAMAC by a 12K PDP8. If a second beam particle (S1S2S3) occurred within 2 μsecs, a bit was set in the status register and the data ignored by the computer. Otherwise the computer stored the data on DEC tape and carried out a preliminary analysis on line. The latter permitted us to show how well particle masses could be separated even without calibration corrections.

3. CALIBRATION

The calibration was performed in two stages. First, non linear effects in the ADCs were determined by observing test pulses of known relative amplitudes. The amplitude of the test pulses was controlled by a power supply whose value was observed with a digital voltmeter. The non-linearity and pedestal current variation of each channel + ADC were determined individually (Fig. 2a) and used to convert all observed ADC bin numbers to a scale linear in input pulse height. Second, this linear scale was converted into energy units using the known energy of the 5.9 KeV Fe^{55} X-ray. These spectra were recorded on DEC tape after every few hundred charged particle events and contain typically 10-20,000 points. A typical spectrum is shown in Fig. 2(b). The peak was determined by a least squares fit of an inverted parabola to the upper half of the main peak. (The calibration was not sensitive to the choice of fitting method.) In this way the major effects of temperature, pressure and gas mixture variation on the gain are corrected. Fig. 2(c) shows to what extent this procedure compensated for gain variations during a particular run. The scatter of points about the line shows that residual gain variations with time are less than 2%. In addition the density of gas appears linearly in the

TABLE I SOURCES OF GAIN VARIATION

	Source	Measurement	Variation	Effect on Gain % (σ)
1.	Drift voltage stability	Digital voltmeter	$<10^{-3}$	
	" " ripple	Oscilloscope	$<10^{-3}$	
				<0.7%
2.	HT wire voltage stability	Digital voltmeter	$<10^{-4}$	
	" " ripple	Oscilloscope	$<10^{-4}$	
				<0.1%
3.	LT power supply and other sources of short term electronic gain variation	Observed dispersion of test pulse response averaged over all channels. Fig. 2(g) shaded spectrum.	$<10^{-2}$	
				<1%
4.	Gas gain variation with time (temp., press. and composition) after correction with Fe data	See fig. 2(c) and text	16×10^{-3}	
				<2%
5.	Gas gain variation along wire	Fe^{55} scan Fig.2(f)	$\lesssim 20 \times 10^{-3}$	
				<2%
	Gain variation from wire to wire	Fe^{55} scan	20×10^{-3}	
				2%
		Charged particles Fig. 2(e)	$<40 \times 10^{-3}$	
				<4%
These include:				
	Wire diameter variation	Laser diffraction	<0.2μm*	
	Signal wire position	Microscope	<8μm	
	High voltage wire position		30μm	∿2%
	Drift electrode position	Capacitor bridge	40μm	∿2%
6.	Random electronic noise	See fig. 2(g)	120 eV/ channel	
			20 eV on mean	1%

* This is a typical figure. The sample of wire actually used has not been measured. Wires tend to have non-circular but relatively uniform cross-sections.

ionisation loss. The temperature and pressure readings from the probes were used to correct all ionisation data to NTP. Various sources of error are discussed in Table I.

The non-linearity of the ADC has already been discussed and calibrated out. Fig. 2(d) shows the non-linearity of the amplification beyond the range used (shaded). There is no serious saturation in either the electronic or gas amplification stages in the range used. The observed non-linearity above 10 KeV is consistent with the expected electronic saturation. The effect of self triggering on the observed pulse height was negligible in the case of Fe spectra where only the "escape peak" was affected. In the case of the charged particles two channels in coincidence were used for the trigger but only one was recorded. This one was observed to be biassed against low pulse heights due to the finite discriminator level (peak labelled "trig" in Fig. 2(e)). This effect may neglected when taken with the other 57 channels. Fig. 2(e) also shows the gain variation from channel to channel observed with the charged particles. The data have statistical errors of order 2% and are not inconsistent with the gain variations observed with an Fe^{55} source and those expected from the mechanical tolerances of the chamber construction (Table I). Fig. 2(f) shows the gain variation along typical wires which is also small. These variations are relatively unimportant since they are the same for every particle and therefore do not contribute towards the overall mass resolution based on the 58 samples. Fig. 2(g) shows the spread of observed test pulse response which is primarily due to electronic noise on a single channel. This interpretation is confirmed by the effect of averaging over all channels for each test "event" when the width is significantly reduced (shaded spectrum).

At each momentum the particle selection was changed several times during a run so that data for the different masses were interleaved. Table II shows the different runs that were made. The 150 GeV/c runs were taken with a "ping" spill (four 200 μsec bursts per flat top, 20-25 beam particles per burst). The

TABLE II

Data Runs

Momentum	Particle	Spill	Contamination	Cerenkov
150 GeV/c	Proton	"ping"	-	7.1 psia He. Below threshold
"	Pion	"	μ, e	" θ > 5 mr
100 GeV/c	Proton	slow	-	8.5 psia He. Below threshold
"	Pion	"	μ, e	" θ > 5 mr
50 GeV/c	Proton	"	K	7.0 psia He. Below threshold
25 GeV/c	Proton	"	K	11.0 psia He. Below threshold
"	Pion	"	μ	θ < 5 mr
"	Electron	"	μ	θ > 5 mr

other momenta were taken with ∿15 triggers per flat top. In every case the selected particle flux exceeded 20% of the beam (S1S2S3). The only significant source of contamination may be the presence of muons among the 25 GeV/c "electrons". The marked difference observed in ionisation between pions and "electrons" shows that this contamination is not dominant. In all other cases the contamination is either very small (<5%) or of no consequence (muons amongst pions).

4. INTERCHANNEL CORRELATIONS

The presence of coupling between channels is shown in Fig. 3, where we have taken the spectra observed for 25 GeV/c electrons as an example. Fig. 3(a) shows how the energy loss observed on a channel depends on whether the

nearest-but-one neighbour was above or below average pulse height. It is seen that it does not. The same is true for protons and pions at 25 GeV/c. The very small shaded peak in the overflow region is not inconsistent with the number of δ-rays of range >3 cms expected.[5] These would give rise to such a positive crosstalk unless multiply scattered away from the parent track (i.e. outside the integration gate). The effect is not large compared with 1%. Fig. 3(b) shows the same data for nearest neighbour channels. A significant negative cross-talk is observed as expected from capacitative effects[4]. Defining the cross-talk parameter, α, in terms of the charges collected, E_i, on each channel, i, and the pulse heights observed ε_i:

$$\varepsilon_i = \alpha E_{i-1} + E_i + \alpha E_{i+1}, \qquad (1)$$

we have simulated this crosstalk in a Monte Carlo calculation using the theoretical dE/dx distribution discussed in paper I[1] and find a best value of:

$$\alpha = -0.055 \pm 0.01$$

The result is given by the smooth curve in Fig. 3(b). The same value of α provides a good fit for 25 GeV/c pions and protons, where the same phenomenon is observed. Indeed observation on an oscilloscope of a dummy (thick wire) channel without gas gain showed these small positive going pulses in coincidence with the negative pulses on the other amplifying channels. The net result of this effect is a small loss of signal amplitude and a change in the shape of the expected energy loss distribution as shown in Fig. 3(c).

A more serious problem was the effective DC level shift observed through the combined effect of all channels capacitatively coupling to the common drift electrodes. In the absence of sufficient capacity in parallel with the drift voltage supply this produced a shift of the zero proportional to the mean pulse height. Since the effect was linear it may be described by a single proportionality constant for the whole experiment, β.

TABLE III

ATOMIC CONSTANTS USED IN THEORETICAL CALCULATION

(ref. 6)

80% Argon/20% CO_2 at NTP ($\hbar\omega_p$ = 0.835 eV)

Argon	K shell	3196.0 eV	2 electrons per argon atom
	L shell	294.0	8
	M shell	39.5	8
Carbon	K shell	313.0	2 electrons per CO_2 molecule
	L shell	55.8	2
		17.7	2
Oxygen	K shell	575.0	4 electrons per CO_2 molecule
	L shell	54.4	4
		39.4	8

Note: The predictions depend only logarithmically on the energy levels assumed.

Extending equation (1) we approximate:-

$$\epsilon_i = \alpha E_{i-1} + E_i + \alpha E_{i+1} - \beta \bar{S}$$

where $\bar{S}$ is a suitably defined mean ionisation for a particular particle velocity.

Comparing our 8 runs with theory we determined $\beta = 0.20 \pm 0.04$ or $\beta\bar{S} \sim 400 \pm 80$ eV*.

* These effects may be avoided by (1) increasing the capacity in parallel with the chamber (2) decoupling the input of the preamplifier to the cathode wires so that changes of drift field are rejected as a common mode signal (3) moving the drift

(We have defined $\bar{S}$ as the peak of the distribution of means of the lowest 35 out of 58 signals as determined by theory. The value of $\beta\bar{S}$ is independent of this choice.)

Together with the uncertainty of its recovery characteristics this effect dominated the systematic errors in this experiment. It was probably responsible for the observation of small anomalous positive correlations between neighbouring channels at 150 GeV/c where the instantaneous particle flux was high. Data for 100 GeV/c π and 50 GeV/c protons also showed the effect. This problem was clearly instrumental since it was not observed in any of the 25 GeV/c runs which spanned the velocity range of the experiment.

5. RESULTS

We have calculated theoretical dE/dx spectra for 1.5 cms of argon/20% CO_2 at NTP according to the method described in paper I[1]. The ionisation potentials and plasma frequency used are given in Table III. These spectra have been further modified by including the 5.5% crosstalk between nearest neighbours and a resolution function with $\sigma \sim 10\%$*. The latter has a negligible effect on the broad spectra. In comparing these spectra with experiment we assume of course that an observed pulse height is directly related to the arrival of a certain number of ionisation electrons at the wire and that this in turn is proportional to the actual energy loss of the primary particle and that the proportionality is the same for the pulse height observed from the X-ray source (5.9 KeV). While this assumption is indefensible in detail it has always been found to work in practice in a statistical sense[8]. Fig. 4 shows the 8 spectra compared with the experimental data in which all 58 channels for each event are shown in the same histogram. The zeroes of the experimental spectra have been shifted as described in the previous section.

---

* This is made up of electronic noise, statistical fluctuations in the number of electrons collected for a given energy loss (Ref. 7) and fluctuations in the gas amplification process.

The value of β in equation 2 is the only free parameter in the comparison. We note that the agreement for protons, pions and electrons at 25 GeV/c is really quite good. On the other hand the comparison with the pion data at 100 GeV/c and 150 GeV/c is much weaker.

In Fig. 5 we show a superposition of the spectra for pions and protons at 25 GeV/c. This makes it clear that no useful information on particle identification is achieved by one or even a small number of measurements on each track. It also shows the long "Landau tail" which prevents the use of a simple "mean ionisation" estimator from resolving the masses. In this experiment 58 measurements are in fact available on each track. To remove the effect of the tail we may discard the largest 23 pulse heights (40%) in each case[1]. The dotted line in Fig. 5 shows the distribution of the remaining 35 pulse heights for each proton event - it has no "Landau tail". If therefore we take the mean of this set of 35 pulse heights for each beam particle we may resolve the pions and protons. Fig. 6 shows a polaroid shot of an on-line display showing the separation of pions and protons achieved in this way using raw data. The origin is some 40 bins off-scale to the left. The separation is on the order of a full width at half maximum (FWHM). Note that the distributions have gaussian shape without tails. Without the zero shift and its related noise the resolution would be much better. Since the shift is proportional to the total energy loss in 1.2 metres of gas, the Landau fluctuations ($\sim$50%)[11] on this represent the main contribution to the loss of resolution.

We have analysed each run in terms of the mean of the lowest 35 pulse heights. The results are given in Table IV together with the equivalent Monte Carlo predictions. Fig. 7 shows the theory and data corrected for the DC shift. The difference between the theoretical and experimental widths shown in Table IV is accounted for by the Landau fluctuations on the shift ($\sim$90 eV RMS). We quote conservative errors of 4% on the means in view of the uncertainties surrounding the shift.

Table IV

THE MEAN OF THE LOWEST 35 OUT OF 58 x 1.5 cms SAMPLES

Argon + 20% CO_2 at NTP

c	Run	Number of Events	Experimental Distribution Before Shift Mean	Width (RMS)	Experimental Mean After Shift ($\beta\bar{S}$)	Monte Carlo Mean	Width (RMS)
6	Protons at 25 GeV/c	1263	1856	168	2244 ± 90	2126	115
2	50 GeV/c	1521	1922	186	2324 ± 93	2319	124
	100 GeV/c	2473	2033	180	2458 ± 98	2485	134
	150 GeV/c	4969	2165	186	2617 ± 105	2554	134
	Pions at 25 GeV/c	1968	2182	176	2638 ± 106	2626	138
	100 GeV/c	2381	2173	196	2627 ± 105	2779	144
0	150 GeV/c	5568	2322	198	2809 ± 110	2798	152
00	Electrons at 25 GeV/c	2114	2282	183	2759 ± 110	2820	158

All energies in electron volts.

Although the possibility of some muon conatmination of the 25 GeV/c electrons cannot be ruled out, the electron data are compatible with the 150 GeV/c pion data. Similarly, there is consistency between the data for 150 GeV/c protons and 25 GeV/c pions. Only the data point for 100 GeV/c pions appears significantly out of line. We note that the relativistic rise is 55 ±4% and that the Fermi plateau extends from p/mc = 500 or so upwards.

Different experimenters work with different gas mixtures, gas thicknesses and statistical methods. In spite of this in Fig. 8 we attempt to compare the ionisation data available[10-12] with the Monte Carlo prediction and curve calculated on the basis of reference 6. The latter and the data of the other experiments refer to the most probable energy loss. Further, all other data above p/mc = 150 were taken with electrons. In spite of this there is general agreement between the data points of this experiment, earlier experiments and the Monte Carlo calculation. All are in disagreement with the Sternheimer curve.

6. CONCLUSION

The results of the Monte Carlo calculation of energy loss in thin gas samples are in good agreement with the data for values of p/mc from 26 to 1000 in argon/20% CO_2 at NTP. Above 1000 the observed energy loss of pions does not differ significantly from electrons since the bremstrahlung probability in a thin gas sample is small and the electromagnetic field of the incident particle has reached its asymptotic form (Fermi plateau)[9]. The resolution of the experiment was limited by instrumental effects which can be avoided in future devices. Nontheless on-line separation of pions and protons at 25 GeV/c was obtained* and there seems to be no reason in principle why very much better separation cannot be achieved with improved systematics and more samples. Finally, we note that

---

* Separation at 9 GeV/c has been achieved previously using a 2.5 m detector (see Ref. 11).

our results are in agreement not only with our calculations by also with the size of the relativistic rise measured by others in gas samples defined by thin windows. This argues against the speculation of Garibyan and Ispiryan[13] that the disagreement with calculations is due to the effect of the windows. This experiment shows that there is no disagreement with calculation and also that the same results are obtained without windows.

ACKNOWLEDGMENTS

We would like to express our thanks for the enthusiastic cooperation and help given us by the Fermi National Accelerator Laboratory and for the support of the experiment by the Science Research Council (UK). We also thank Roger Giles, Mike Walker, Mick Flinn and the Oxford Nuclear Physics main workshop for their part in building the chamber; finally we are grateful to Peter Shield for designing and building most of the electronics.

REFERENCES

1. The ionisation loss of relativistic charged particles in thin gas samples and its use for particle identification: I, theoretical predictions. J.H. Cobb, J.N. Bunch, W.W.M. Allison (previous paper).

2. W.W.M. Allison et al, NIM 119, 499 (1974).

3. J.H. Cobb, D. Phil. thesis, University of Oxford (1975). Available from Rutherford Laboratory, HEP/T/55.

4. G. Charpak, Ann. Rev. Nucl. Sci. 20, 226, (1970).

5. J.L. Lloyd and A.W. Wolfendale, Proc. Phys. Soc. 73, 178 (1959).

6. R.M. Sternheimer and R.F. Pieirls, Phys. Rev. 88, 851 (1952) and Phys. Rev. B3, 3681 (1971).

7. See Ref. 4 page 232.

8. Methods of Experimental Physics Vol. 5A, Yuan and Wu (Eds.) Academic Press (1961) page 43.

9. O. Blunck and K. Westphal, Zeit. für Phys. 130, 641 (1951).

10. P.V. Ramana Murthy, NIM 63, 77 (1968).

11. D. Jeanne et al., NIM 111, 287 (1973); M. Aderholz et al., NIM 118 419 (1974).

12. F. Harris et al, NIM 107, 413 (1973).

13. G.M. Garibyan and K.A. Ispiryan, JETP Letters 16, 585 (1972).

FIGURES

Fig. 1

(a) Beam diagram

(b) Schematic side view of proportional chamber

(c) Top view of chamber and amplifier box

(d) View of chamber in beam direction

(e) Picture showing details of plane construction

Fig. 2

(a) Non-linearity of a typical ADC. The pedestal current was large so that only the shaded more linear region was used.

(b) A typical Fe^{55} spectrum taken during part of a run between accelerator cycles.

(c) The relative gain variation during a run as measured by Fe^{55} X-ray pulse heights plotted against the relative gain variation as measured by charged particle mean pulse heights. The line indicates the expected correlation.

(d) Linearity of amplification (gas + electronic) as shown by various X-ray sources. The dynamic range of the 8 bit ADCs were matched to the shaded region.

(e) Variation of channel gain attributable to variations in gas amplification from wire to wire (charged particle data with statistical error 2%). See table I.

(f) The gain variation along wires measured by scanning an Fe^{55} source through the operating region.

(g) The spread of test pulse response due to electronic noise on a single channel. Shaded spectrum is the same averaged over all channels.

Fig. 3

The difference in energy loss spectra due to near neighbour cross talk. The upper histogram in (a) and (b) shows the spectrum on a channel when the near neighbour pulse height is small and the shaded spectrum shows how much this changes when the near neighbour is large.

(a) For second nearest neighbours (25 GeV/c e^-).

(b) For nearest neighbours. (25 GeV/c e^-)

The smooth curve shows the expected result for $\alpha = -0.055$.

(c) Shows the effect on the theoretical dE/dx distribution of folding in crosstalk of -5.5% (for 25 GeV/c protons).

Fig. 4

The dE/dx spectra for the 8 different velocities measured, corrected to NTP and including correction for the zero shift. The theoretical curves include the effect of the 20% CO_2, the -5.5% nearest neighbour crosstalk and a small effect due to statistics of the electrons (assumed Poisson). The ordinate of the histograms is the number of samples per 100 eV energy bin. The normalisation in each case is 58 times the number of events quoted in Table IV.

Fig. 5

A superposition of the distributions of all channels for π and p at 25 GeV/c. The dashed histogram shows the effect on the proton distribution of histogramming only the smallest 35 out of 58 pulses recorded in each event.

Fig. 6

A polaroid shot showing the separation of pions and protons at 25 GeV/c achieved by the on-line PDP8 programme working with raw data. Each point in

Fig. 6 (cont.)

the two histograms refers to a single beam track with a value equal to the mean pulse height after discarding the largest 23 pulses. The origin is off scale to the left. The last column of Table IV shows that much better separation may be expected in the absence of systematic effects (see text).

Fig. 7

A comparison of the relativistic rise of the mean of the lowest 35 out of 58 x 1.5 cm samples with theory for argon/20% CO_2 at NTP.

Fig. 8

Compilation of world data on the relativistic rise in argon as measured in proportional chambers. The dashed curve refers to a calculation according to the prescription of Ref. 6. The solid curve is discussed in the text. The comparison is essentially qualitative as the various experiments and calculations relate to different quantities and different gas mixtures.

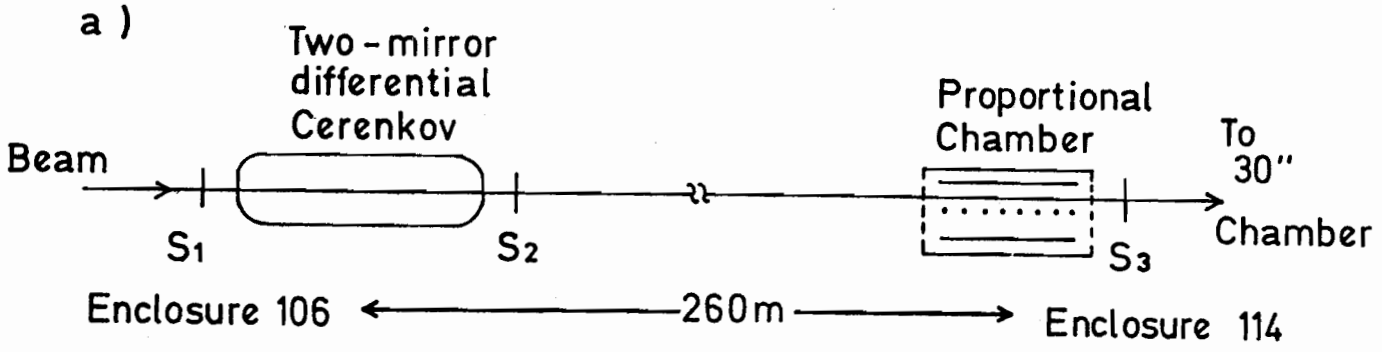

BEAM DIAGRAM

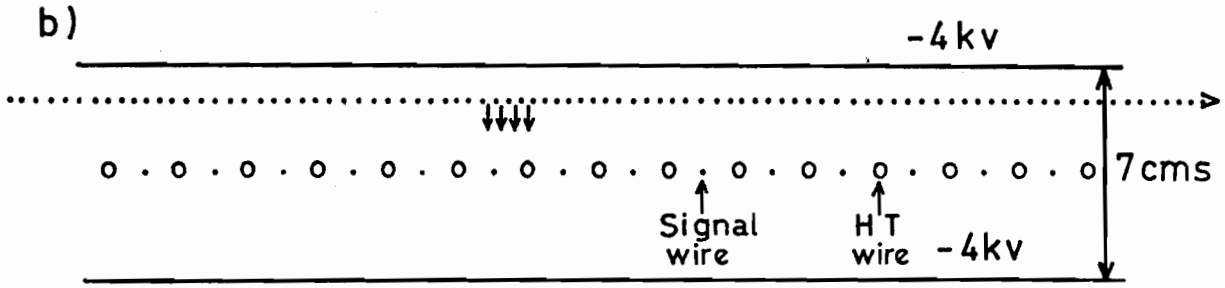

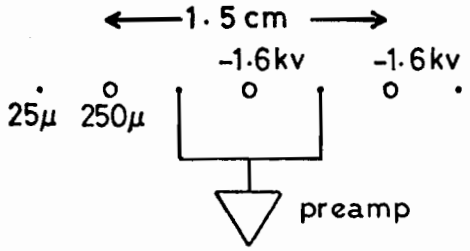

SCHEMATIC SIDE VIEW OF PROPORTIONAL CHAMBER

Fig. 1

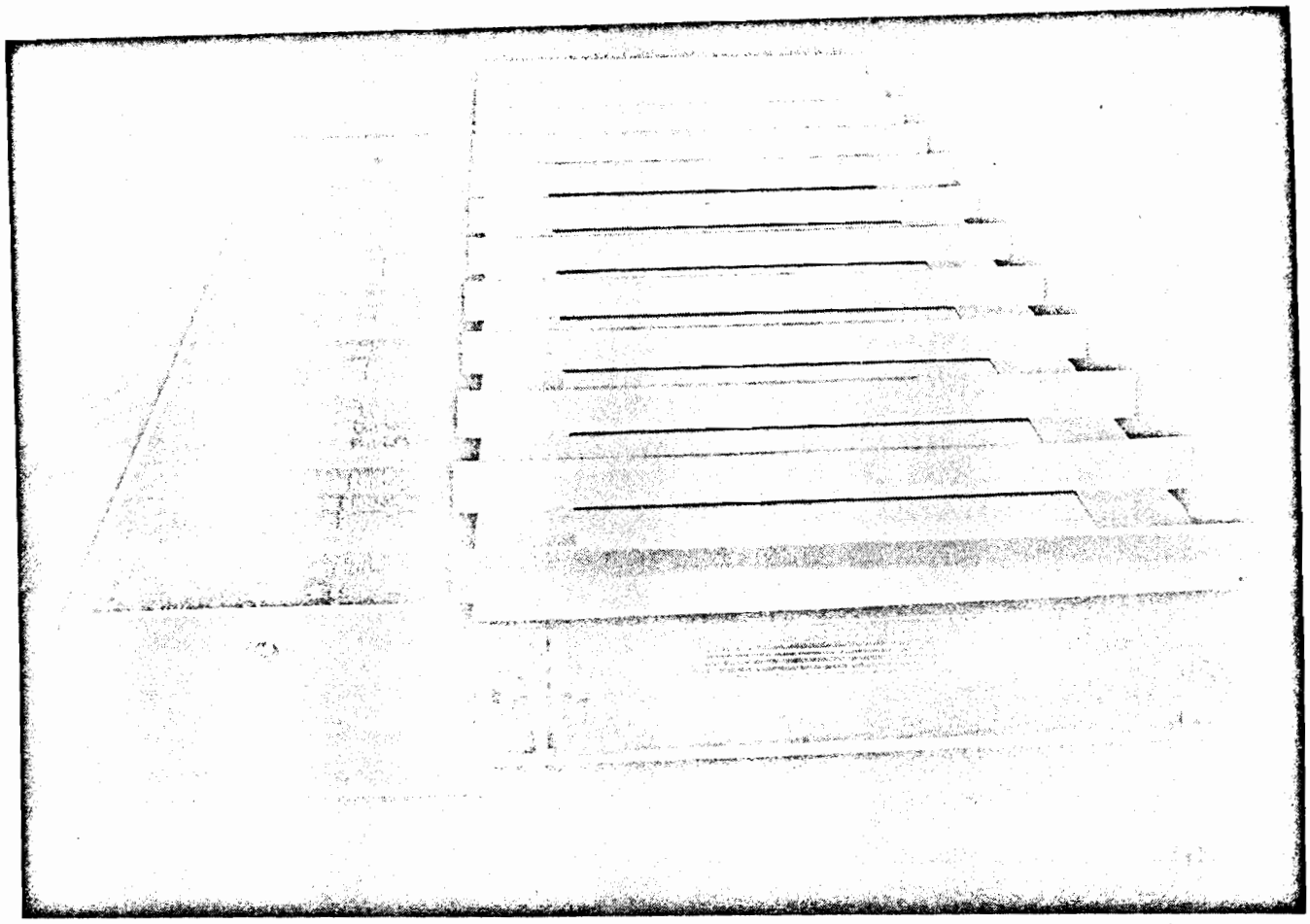

Fig. 1c

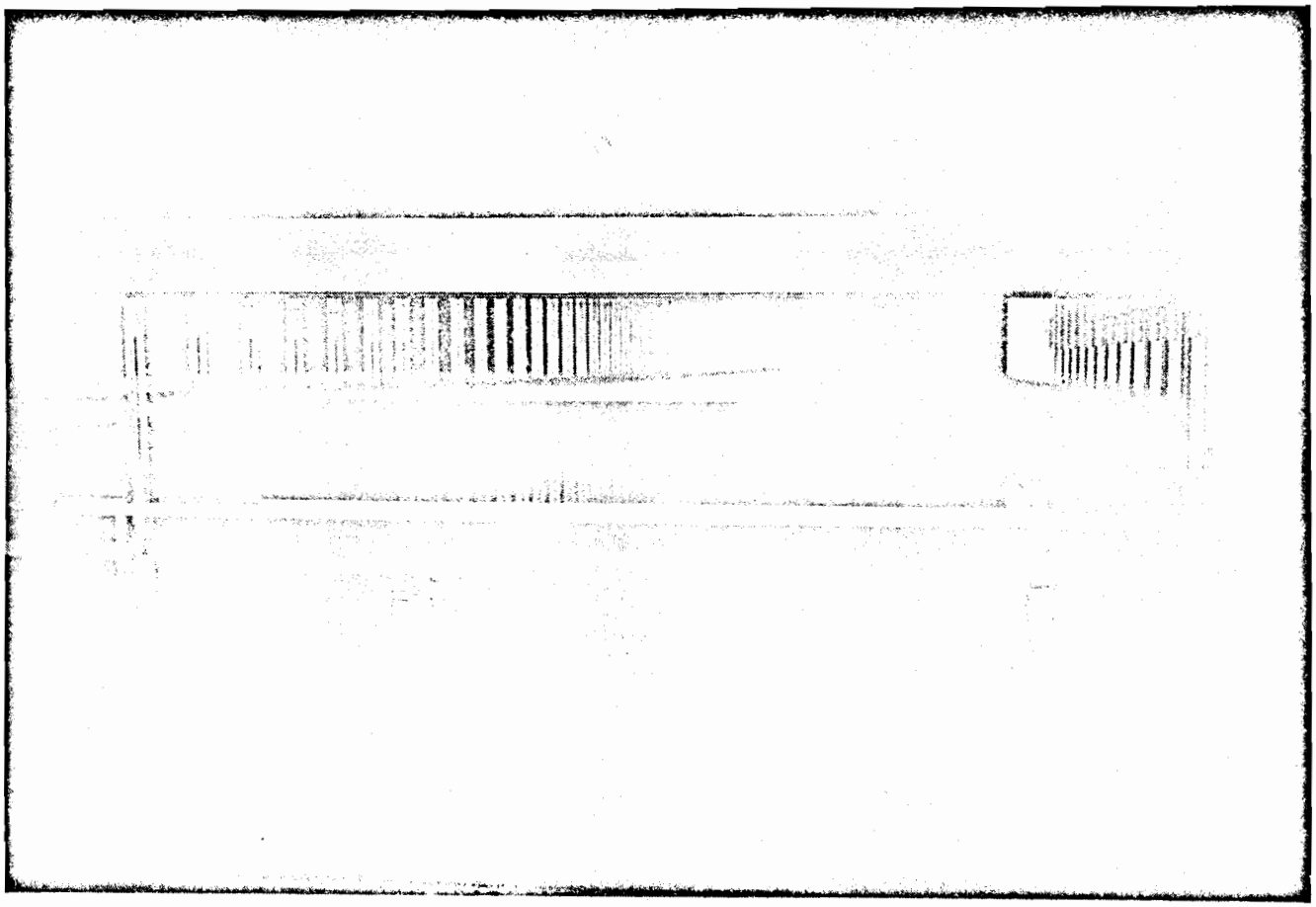

Fig. 1d

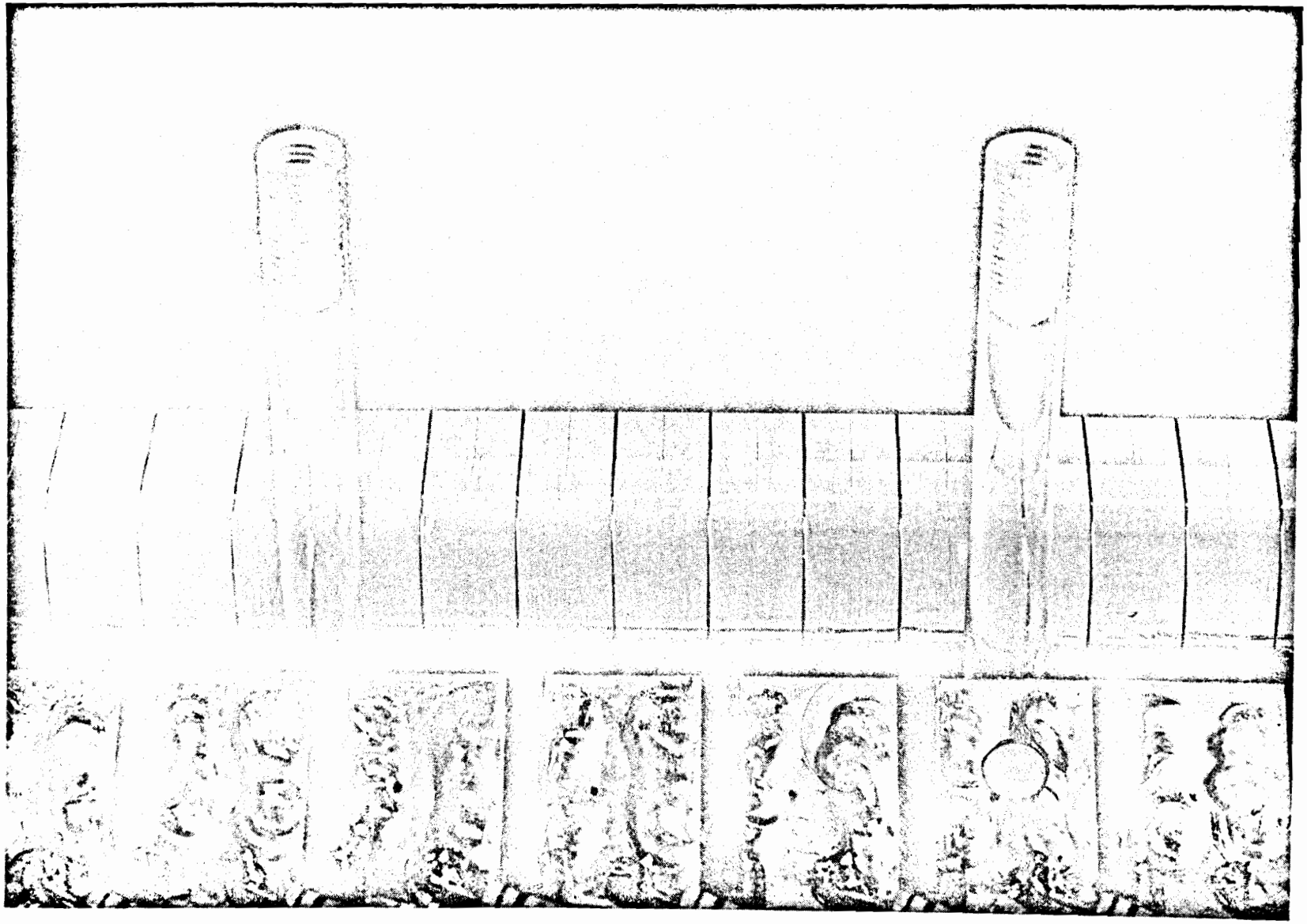

Fig. 1e

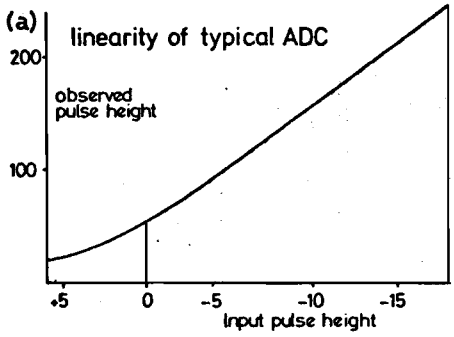
(a)
linearity of typical ADC
200
100
observed pulse height
+5
0
-5
-10
-15
Input pulse height

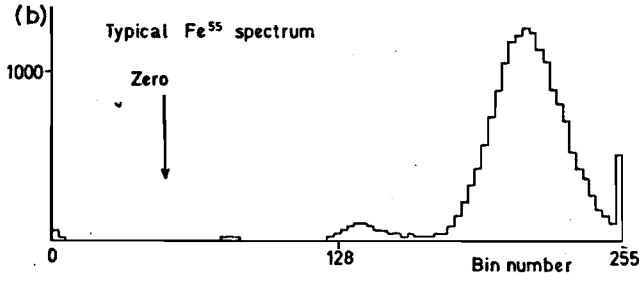
(b)
Typical Fe55 spectrum
1000
Zero
0
128
Bin number
255

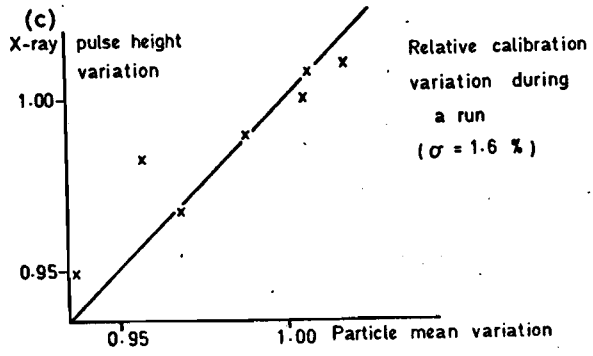
(c)
X-ray pulse height variation
1.00
0.95
0.95
1.00 Particle mean variation
Relative calibration variation during a run
(σ = 1.6 %)

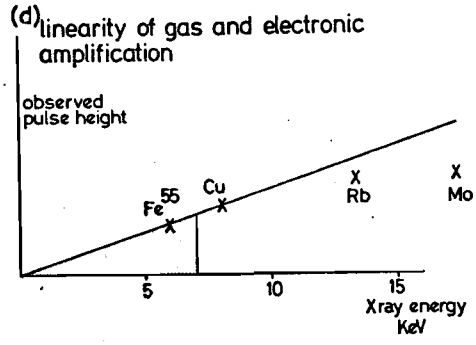
(d) linearity of gas and electronic amplification
observed pulse height
Fe55
Cu
Rb
Mo
5
10
15
Xray energy KeV

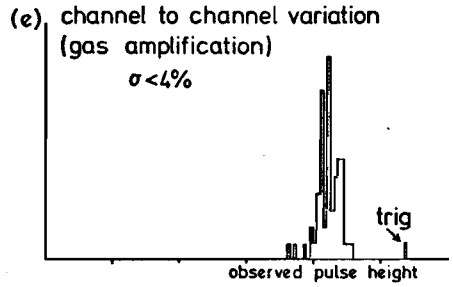
(e) channel to channel variation
(gas amplification)
σ<4%
trig
observed pulse height

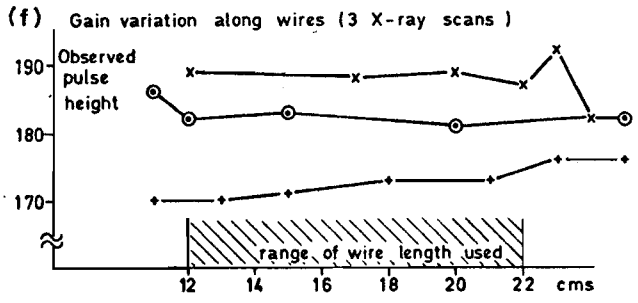
(f) Gain variation along wires (3 X-ray scans)
Observed pulse height
190
180
170
range of wire length used
12
14
16
18
20
22
cms

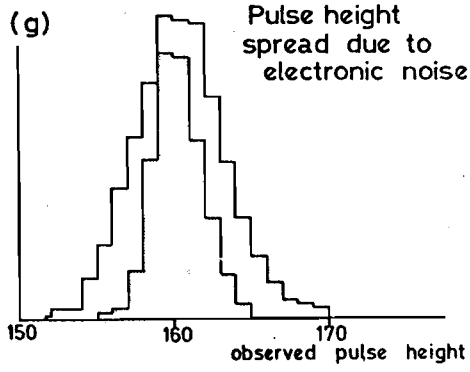
(g)
Pulse height spread due to electronic noise.
150
160
170
observed pulse height

Fig. 2

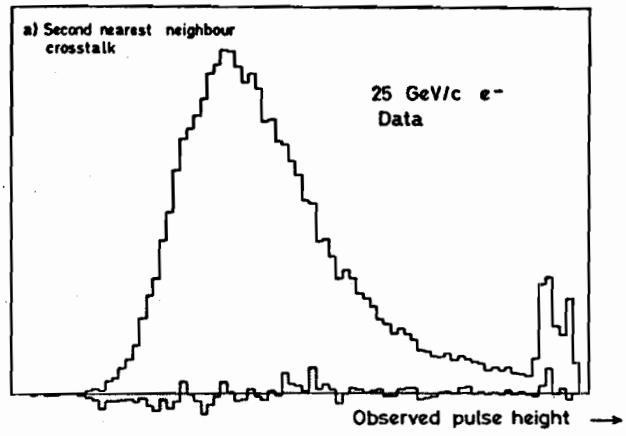

Fig. 3a

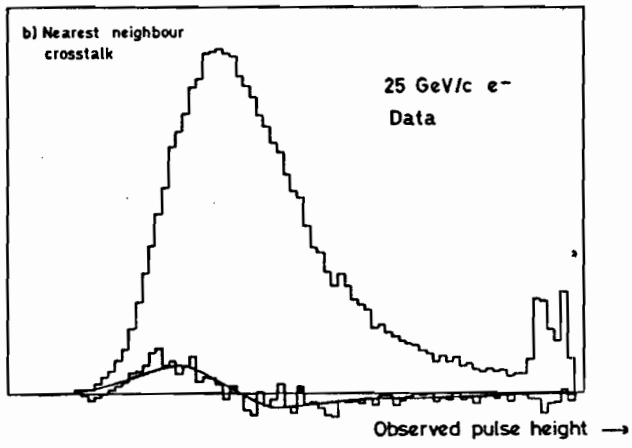

Fig. 3 b

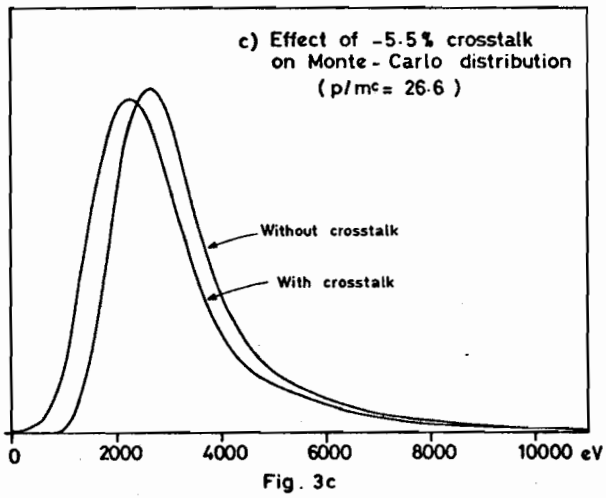

Fig. 3c

Fig. 3

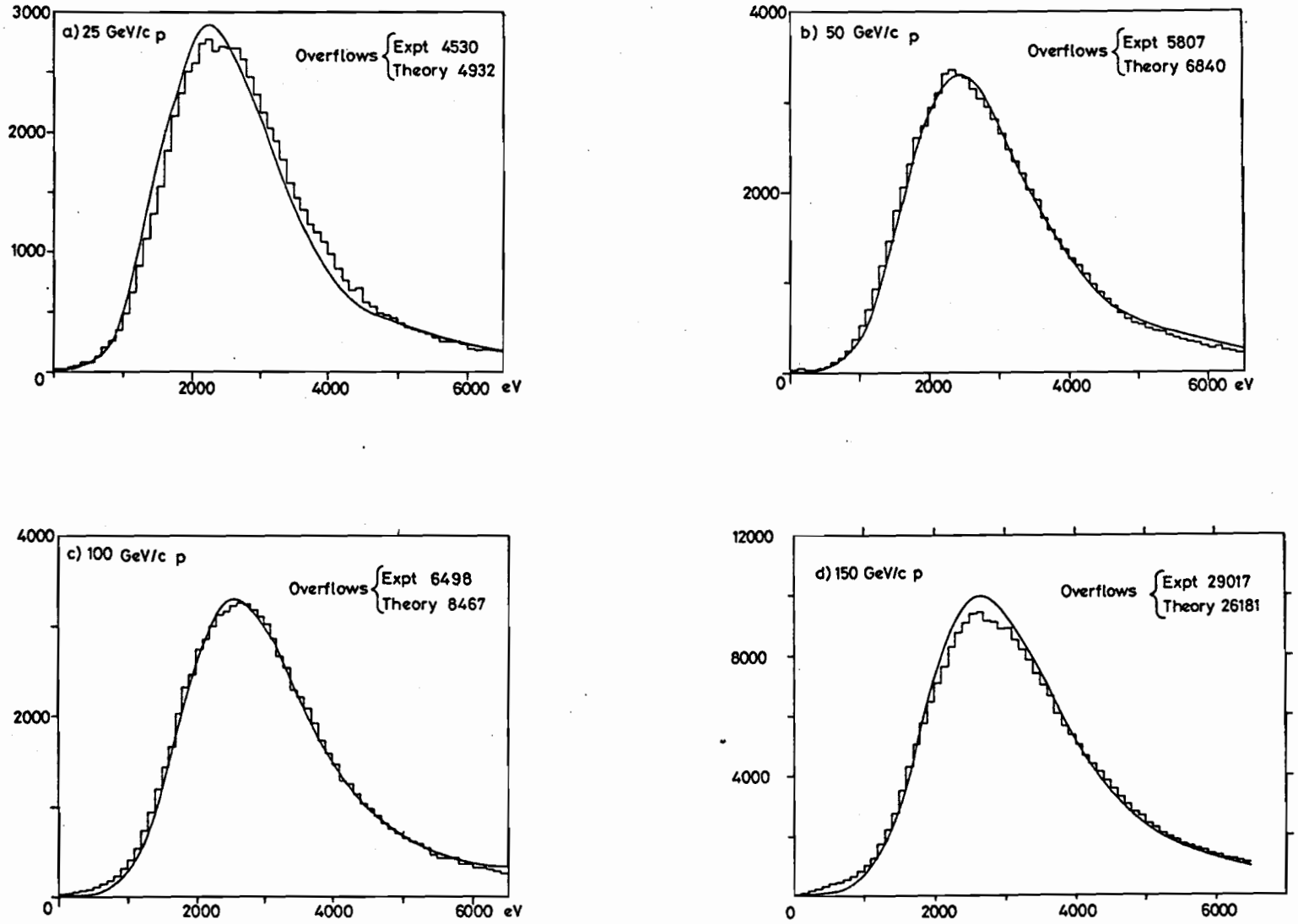
a) 25 GeV/c p
Overflows {Expt 4530
Theory 4932
3000
2000
1000
0
2000
4000
6000 eV
b) 50 GeV/c p
Overflows {Expt 5807
Theory 6840
4000
2000
0
2000
4000
6000 eV
c) 100 GeV/c p
Overflows {Expt 6498
Theory 8467
4000
2000
0
2000
4000
6000 eV
d) 150 GeV/c p
Overflows {Expt 29017
Theory 26181
12000
8000
4000
0
2000
4000
6000

Fig. 4

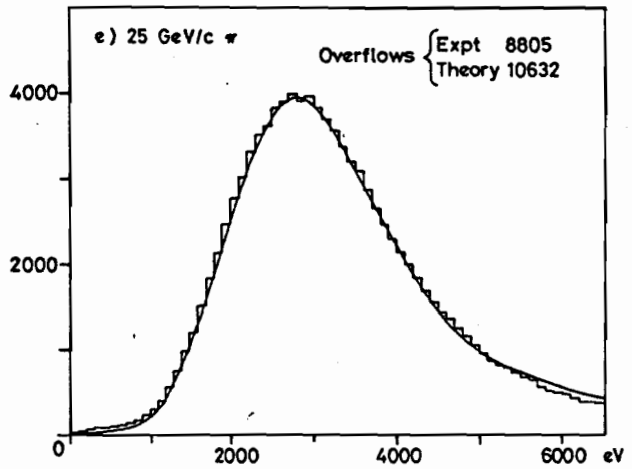
e) 25 GeV/c π
Overflows {Expt 8805
Theory 10632
4000
2000
0
2000
4000
6000 eV

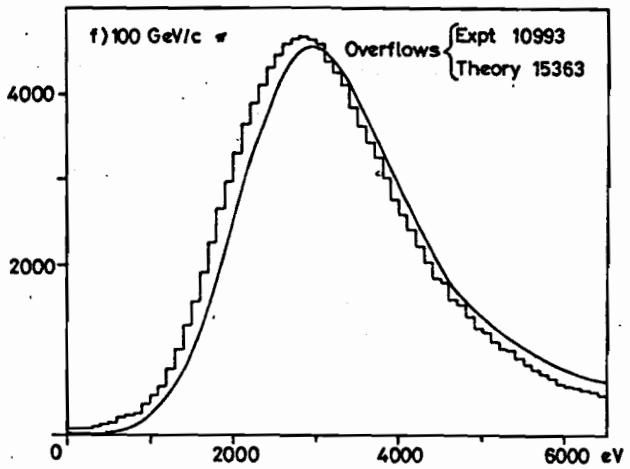
f) 100 GeV/c π
Overflows {Expt 10993
Theory 15363
4000
2000
0
2000
4000
6000 eV

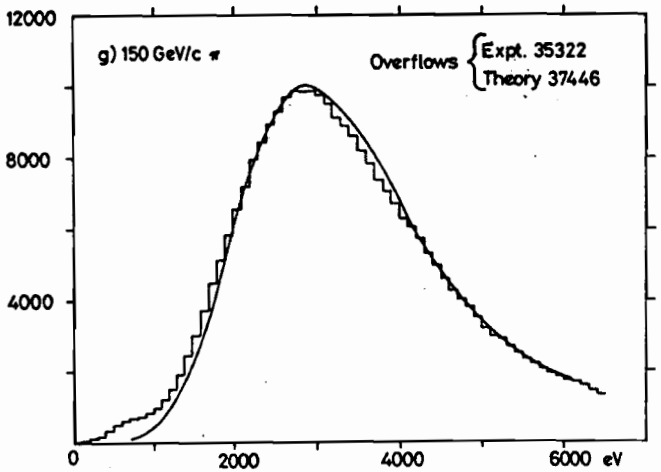
g) 150 GeV/c π
Overflows {Expt. 35322
Theory 37446
12000
8000
4000
0
2000
4000
6000 eV

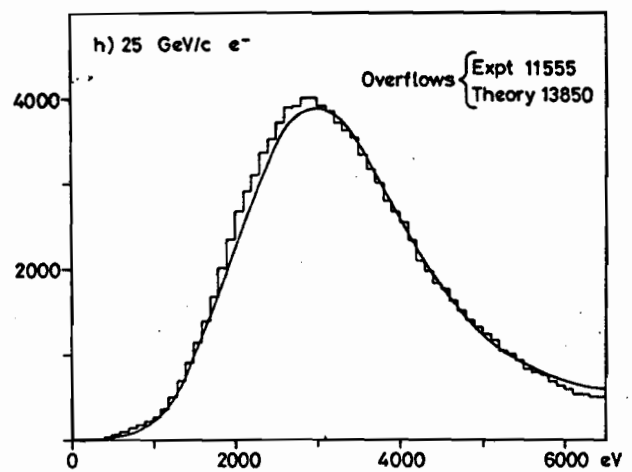
h) 25 GeV/c e⁻
Overflows {Expt 11555
Theory 13850
4000
2000
0
2000
4000
6000 eV

Fig. 4

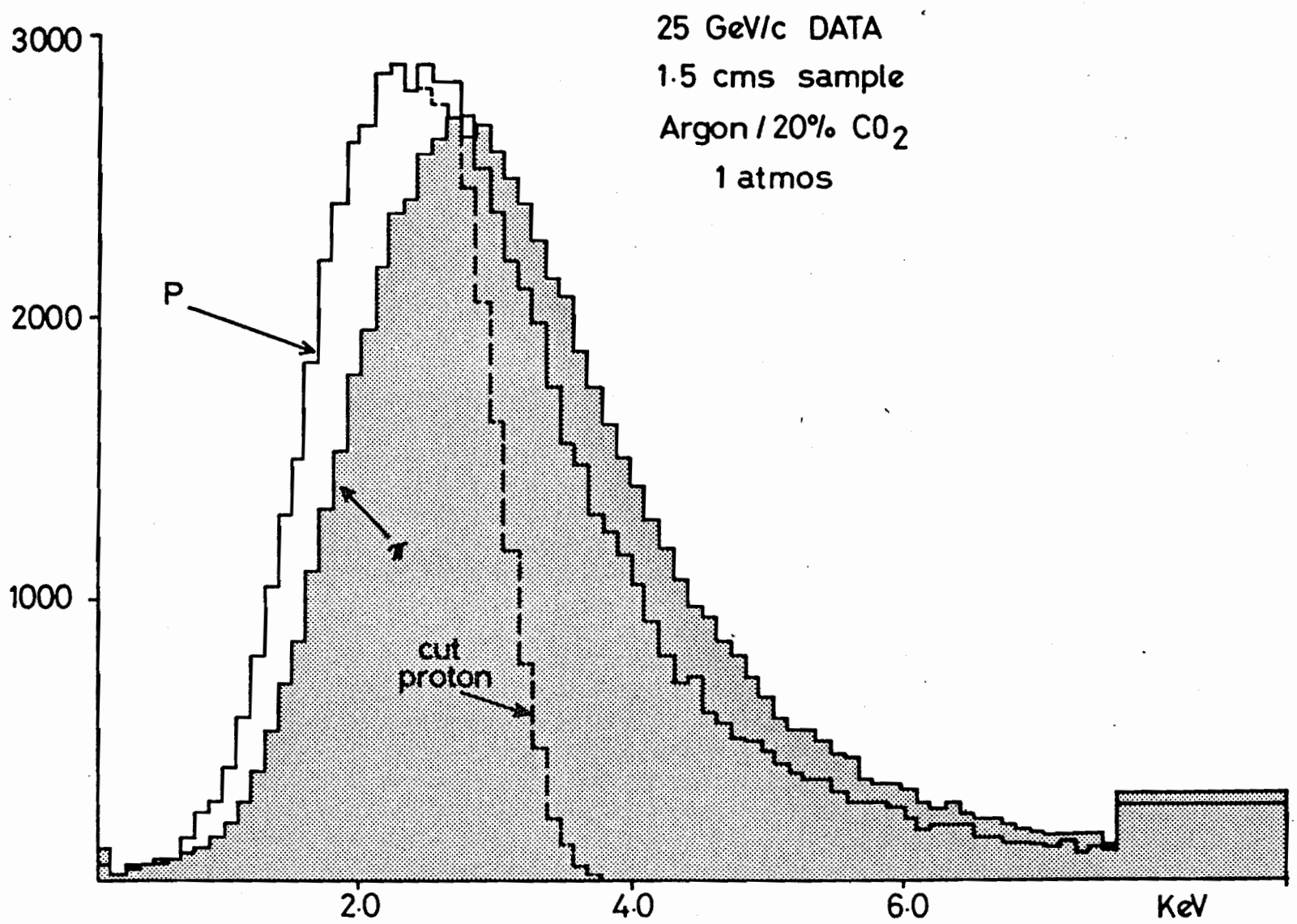
25 GeV/c DATA
1·5 cms sample
Argon / 20% CO_2
1 atmos
3000
2000
1000
P
π
cut
proton
2·0
4·0
6·0
KeV

Fig. 5

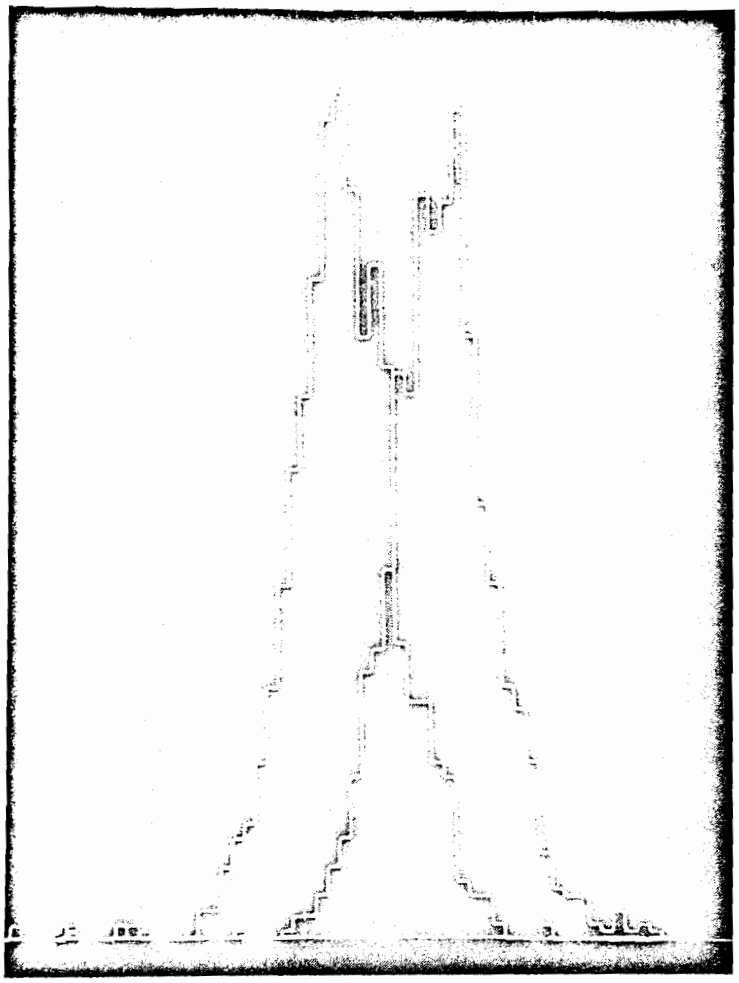

Fig. 6

Fig.7

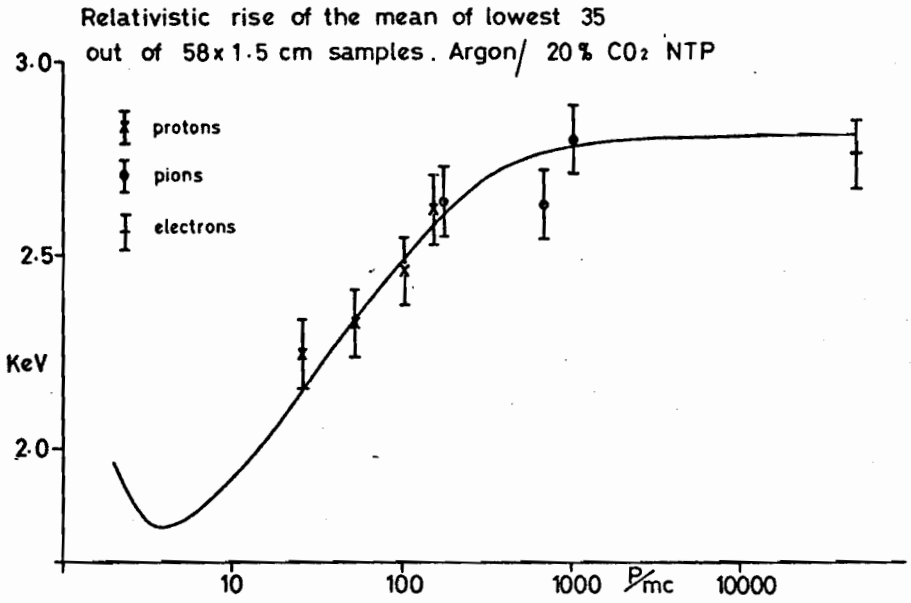
Relativistic rise of the mean of lowest 35
out of 58 x 1.5 cm samples. Argon/ 20% CO2 NTP
protons
pions
electrons
3.0
2.5
2.0
KeV
10
100
1000
P/mc
10000

Fig.8

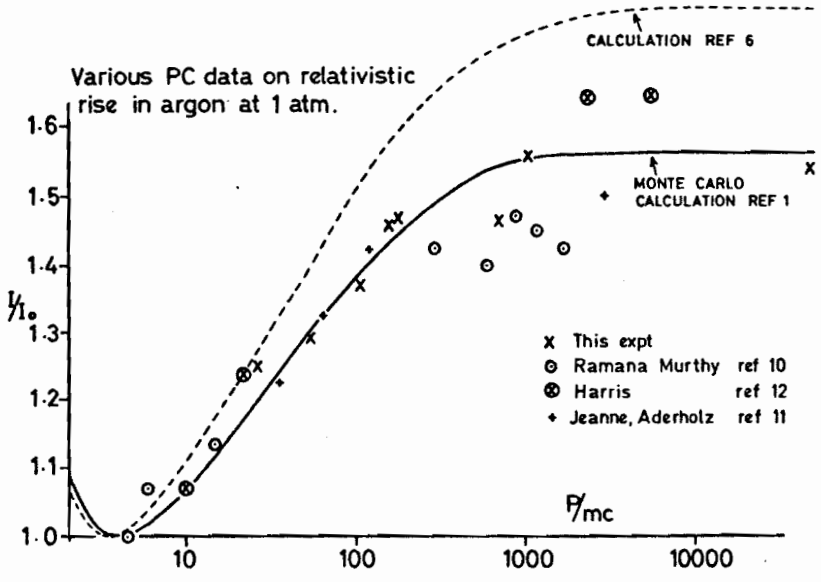
Various PC data on relativistic
rise in argon at 1 atm.
CALCULATION REF 6
MONTE CARLO
CALCULATION REF 1
This expt
Ramana Murthy ref 10
Harris ref 12
Jeanne, Aderholz ref 11
I/I0
1.6
1.5
1.4
1.3
1.2
1.1
1.0
10
100
1000
10000
P/mc